

Modeling and Characterization of Metastability in Single Flux Quantum (SFQ) Synchronizers

Gourav Datta, Peter A. Beerel

Ming Hsieh *Department of Electrical and Computer Engineering*

University of Southern California

Los Angeles, California 90089, USA

{gdatta, pabeerel}@usc.edu

Abstract—Despite the promises of low-power and high-frequency of single-flux quantum (SFQ) technology, scaling these circuits remains a serious challenge that motivates the support of multiple SFQ clock domains. Towards this end, this paper analyzes the impact of setup time violations and metastability in SFQ circuits comparing the derived analytical models to their CMOS counterparts. It then extends this model to estimate the Mean Time Between Failure (MTBF) of flip-flop-based synchronizers and curve fits this model to simulations in the state-of-the-art SFQ5ee process. Interestingly, we find a two-flop SFQ synchronizer has an estimated MTBF of $\sim 10^6$ years.

Index Terms—SFQ, metastability, synchronizers, Mean Time Between Failure.

I. INTRODUCTION

With CMOS technology facing increased challenges due to the limits of physical scaling [1], superconductive digital electronics (SDE), especially single flux quantum (SFQ) [2], has appeared as a promising beyond-CMOS device technology supporting frequencies up to 370 GHz [3] and yielding switching energy per bit of $10^{-19} J$ at $T = 4.2 K$ (liquid helium temperature) [4], [5]. Recently, several variants of SFQ technologies with even higher energy efficiency have been demonstrated [6]–[10]. Still, the promise of three orders of magnitude lower in power (in the case of non-resistive bias networks [6]) at an order of magnitude higher frequency [2], has not yet been attained, primarily due to i) high process variations [11], [12], ii) the lack of a compact and reliable memory element and controllable switch element, and iii) the lack of design automation methodologies and techniques that enable the design of large-scale SFQ circuits.

In particular, the ultra-high clock frequencies associated with SFQ makes low-skew clock distribution extremely challenging [13]. As a result, a 1THz device was forced to function at a disastrous 20 GHz frequency [11]. One approach to address this clocking challenge is to decompose the SFQ design into multiple blocks that are independently clocked, i.e., into multiple clock domains, similar to how large CMOS designs are managed. Since these clock domains have no phase relationship, no static timing constraints can be created for data transfer between them. As a result, the timing constraints between the flip-flops (FFs) at the boundary of these domains may be violated and the sampling FF in the receiver domain can exhibit metastability [14].

To reduce the chance of metastable events propagating through a design, designers often use a sequence of back-to-back FFs, called a *synchronizer* [15], [16], whenever data is transferred between unrelated clock domains. Should the output of the first synchronization FF become metastable, it still needs to propagate through the rest of the sequence before its value is used by the rest of the design. The extra amount of time provided by the additional synchronization FFs increases

the probability that the metastable value will resolve, and lowers the possibility that the design will fail [17]. The cost of the synchronizer is that it increases design latency.

This paper analyzes metastability in SFQ circuits and then quantifies it in the form of the Mean Time Between Failures (MTBF) of SFQ synchronizers that consist of a sequence of back-to-back FFs. To the best of our knowledge, we are the first to propose an analytical model of metastability in SFQ. We extract different parameters of this model using circuit simulations to compute MTBF in the current-state-of-the-art SFQ process, SFQ5ee [18]. We then discuss how multi-FF synchronizers can improve this MTBF.

The remainder of the paper is organized as follows. Section II provides related background on SFQ, including a description of a SFQ FF used to store SFQ pulses and metastability in SFQ. Section III derives an analytical model for metastability in SFQ logic circuits. Section IV performs JSIM [19] simulations to generate the model parameters and compute MTBF of different FF-based synchronizers. Finally some conclusions are given in Section V.

II. BACKGROUND

A. SFQ

Unlike in CMOS, in SFQ technology, binary information is represented by very short (picosecond) voltage pulses $V(t)$ of quantized area, corresponding to transition of a single flux quantum, $\phi_0 = \int V(t)dt = \frac{h}{2e} = 2.03 \text{ mV.ps}$. These SFQ pulses can be quite naturally generated, reproduced, amplified, memorized, and processed by elementary cells comprising overdamped Josephson junctions (JJs) [2]. In particular, the DC superconducting quantum interference device (SQUID) is the fundamental structure that is used as a memory element to store SFQ pulses [11] and, to explain its use, we illustrate a SFQ D flip-flop (DFF) along with representative simulation waveforms in Figs. 1(a) and 1(b). The DFF has two stable states, 0 or 1, that are characterized by the direction of the quantized current i_L (one fluxon) in the loop consisting of two JJs, labelled J_1 and J_2 , separated by an inductor L_2 . Depending upon the state of the DFF, the arrival of clock pulse causes either the J_2 to leap (if the state is 1) or J_3 to leap (if the state is 0). If J_2 leaps, an output pulse will be generated losing the fluxon stored in the loop and resetting it to 0 state. On the other hand, if J_3 leaps, no pulse will be generated. J_2 and J_3 together form the Josephson comparator which senses the input current i_L to decide which JJ to leap. Previous work has analyzed the switching characteristics of these comparators [20], [21], but to the best of our knowledge, there is no prior work modeling their output delay.

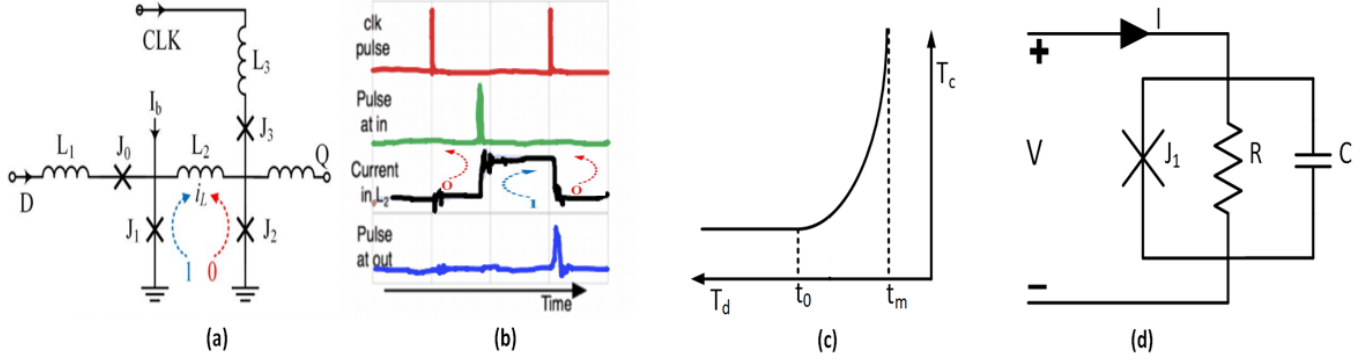


Fig. 1. (a) Schematic of a DFF (b) Simulation result of a DFF in SFQ (c) Illustration of clock-to-Q delay T_c as a function of the arrival time of the data pulse T_d relative to the clock. (d) RCSJ model of J_1

B. Metastability in SFQ (Increased Clock-to-Q Delay)

Because of the quantized nature of SFQ, there is no notion of a metastable voltage and there can never be a runt pulse generated at the output of an SFQ DFF. Either the output generates a pulse with energy of one fluxon or it does not. However, when the input pulse violates the setup time of the DFF, the clock-to-Q delay of the DFF can increase in an unbounded manner (see Fig. 1(c)), similar to what is observed in CMOS and bipolar technologies [22]–[24]*. As a result, this additional delay in the current pipeline stage can bleed into the next stage and cause a setup failure there [22].

In CMOS, the clock-to-Q delay of a DFF accounts for a small portion of the clock period due to the presence of 6+ levels of logic gates [25] in the combinational path. In contrast, in SFQ, each logic gate is clocked, i.e., SFQ is inherently gate-level pipelined. This means that the number of clock sinks is large and the clock-to-Q delay is a dominant factor of their minimum clock period. Clocking is thus very challenging, as SFQ circuits are more sensitive to setup failures that cause increases in clock-to-Q delay than their CMOS counterparts. It is therefore important to model and analyze clock-to-Q delay, particularly in the context of crossing clock domains where setup violations are expected.

III. MODELING METASTABILITY

Let us first introduce a few relevant notations illustrated in Fig. 1(c). We denote the clock-to-Q delay of a DFF as T_c and the time before the clock that the data pulse arrives at a DFF as T_d . We define t_0 as the time of the arrival of the data before the clock when the clock-to-Q delay starts to increase from its' nominal value. We also define t_m , where $t_m \leq t_0$, as the minimum data arrival time before the clock for which the corresponding output pulse is generated in the same clock cycle. Note that the DFF enters a metastable state once the clock pulse arrives if $T_d = t_m$. In this case, the clock-to-Q delay approaches infinity, i.e., the comparator does not know whether to trigger J_2 or J_3 . However, similar to CMOS, any small perturbation will take the DFF out of this state. As a result, it will either trigger J_3 with delaying the output pulse until the arrival of the next clock pulse or J_2 with a high clock-to-Q delay. However, unlike in CMOS, the delayed output pulse will be generated as soon as the next clock pulse arrives, limiting the overall impact of metastability.

*Interestingly, when the output pulse is delayed by a clock, the DFF exhibits the nominal clock-to-Q delay.

Thus, unlike CMOS, the increased clock-to-Q delay is not the length of time the DFF remains in metastability, but instead caused by the superconducting nature of the circuit near the metastable state, i.e., as T_d approaches t_m . This is described in more detail below.

A. Reason for Increased Clock-to-Q Delay

To gain a physical understanding of the relationship between T_d and T_c , we further analyze the SFQ DFF. The output pulse of the DFF is delayed when the junction J_1 does not get enough time to undergo a 2π phase leap and thereby cannot flip the state of the $J_1 - L_2 - J_2$ loop before the arrival of the clock pulse. The time taken by J_1 to flip the state is derived below.

Consider the RCSJ model of J_1 , as shown in Fig. 1(d) with a capacitor (C) and resistor (R) in parallel, the latter acting as a shunt to overdamp J_1 . The total current which is the sum from Kirchoffs' laws is given by

$$I(t) = I_c \sin \phi(t) + \frac{V(t)}{R} + C \frac{dV(t)}{dt} \quad (1)$$

Here, $V(t)$ is the voltage across J_1 and $I(t)$ the total current. I_c and ϕ are the critical current and phase of J_1 respectively. Using flux to voltage conversion in Eq. 2, we obtain the full current equation in Eq. 3.

$$V(t) = \frac{\hbar}{2e} \frac{d\phi(t)}{dt} \quad (2)$$

$$I(t) = I_c \sin \phi(t) + \frac{\hbar}{2eR} \frac{d\phi(t)}{dt} + C \frac{\hbar}{2e} \frac{d^2\phi(t)}{dt^2} \quad (3)$$

which is a second order nonlinear ordinary differential equation. Note that e is the elementary charge and \hbar is the reduced Planck's constant. J_1 is initially biased in superconducting state with $I(t) = I_0$, where $I_c \geq I_0$. Note that I_0 is primarily provided by the bias current source I_b .

The phase $\phi(t)$ in this condition does not change with time.

$$\phi(t) = \phi_0 = \arcsin\left(\frac{I_0}{I_c}\right) \quad (4)$$

and hence, $V(t)$ is zero. With the arrival of the input pulse, $I(t)$ becomes I_1 with $I_c < I_1$, the phase grows with time and we can observe a nonvanishing voltage. The time required to increase this phase by an angle of 2π can result in one quantum flux being stored in the inductance loop. This time is denoted

t_0 . Since we use overdamped JJs in SFQ logic, we can ignore the RC time constant since it is much smaller than the intrinsic time constant of J_1 . With this assumption, we rewrite Eq. 3 ignoring the second order term, as follows,

$$\frac{\hbar}{2eR} \frac{d\phi(t)}{I_1 - I_c \sin \phi(t)} = dt \quad (5)$$

and integrate over a 2π change in $\phi(t)$ to obtain

$$t_0 = \frac{\hbar}{2eR} \frac{2\pi}{\sqrt{I_1^2 - I_c^2}} \quad (6)$$

We can also integrate over an arbitrary time period $(0, T_d)$ with $T_d \leq t_0$ and obtain

$$\phi(T_d) = \begin{cases} 2 \arctan \left(a \cdot \tan \frac{T_d \cdot b}{2\tau} \right) + \phi_0, & \text{if } T_d \leq \frac{\pi\tau}{b} \\ 2 \arctan \left(a \cdot \tan \frac{T_d \cdot b}{2\tau} \right) + \phi_0 + 2\pi, & \text{otherwise} \end{cases} \quad (7)$$

where $\tau = \frac{\hbar}{2eI_c R}$, $a = \sqrt{1 - \left(\frac{I_c}{I_1}\right)^2}$ and $b = \sqrt{\left(\frac{I_1}{I_c}\right)^2 - 1}$. Note that $\phi(T_d)$ is an increasing function in T_d with $\phi(0) = \phi_0$ and $\phi(t_0) = \phi_0 + 2\pi$.

The output clock-to-Q delay is nominal when the input pulse arrives at time $t \geq t_0$. However, any pulse on the data input, if not given time t_0 before the clock, will result in some phase change less than $\phi(t_0)$ across J_1 . Hence, when the clock pulse arrives, the resulting current δI in L_2 will not result in a quantum of fluxon. As a result, the output pulse either comes out with a delay higher than the nominal value, as detailed in the next subsection, or does not come out until the arrival of the next clock pulse.

To be more precise, the output comes out in the next clock cycle, if the pulse on the data input arrives later than t_m . When the input is later than t_m , the resulting current δI produced in L_2 and passed into J_2 (including the shunt resistor and capacitor shown in Fig. 1(d)) becomes less than J_2 's critical current when the clock pulse arrives. Hence, J_3 will leap and no associated output pulse will be generated. However, since the inductance loop stores the flux, once the next clock pulse comes, J_2 will leap resulting in an output pulse. Hence, any late input pulse, specifically after t_m , delays the latency of the output pulse by one clock cycle.

B. Modeling Increased Clock-to-Q Delay

Now, let us derive the temporal dynamics of the response time of the DFF, particularly when the input pulse arrives between t_0 and t_m . Without any input pulse, J_2 is biased at $I_c \sin \theta_0$ (similar to J_1) where θ_0 is the static (superconducting) phase of J_2 . With the 2π phase leap of J_1 and the arrival of the clock pulse, we inject additional current δI_d and δI_{clk} respectively into J_2 , such that $I_c \sin \theta_0 + \delta I_d + \delta I_{clk}$ becomes larger than I_c .

Note that δI is upper bounded by I_{max} which results from a complete 2π phase change in J_1 . Moreover, we can substitute $I = I_c \sin \theta_0 + I_{max} + \delta I_{clk}$ into Eq. 6 to get the nominal clock-to-Q delay of the flop. However, δI_d starts to drop below I_{max} when T_d decreases below t_0 , i.e., violates the setup time of the DFF. This decrease continues until T_d becomes t_m where $I_c \sin \theta_0 + \delta I_d + \delta I_{clk} = I_c$ and T_c approaches infinity.

The phase change across J_1 computed as $\phi(T_d)$ is similar to the angular magnetic flux which is proportional to the current across the inductor L_2 . Therefore, δI_d can be written as $K_1 \phi(T_d)$ with K_1 being an arbitrary constant. Referring to Eq. 6 and linking the change in input current (phase) as a function of time of arrival of the input pulse T_d , the clock-to-Q delay can be modelled as

$$T_c = f(T_d) = \frac{\hbar}{2eR} \frac{2\pi}{\sqrt{(I_x + K_1 \phi(T_d))^2 - I_c^2}} + K_2 \quad (8)$$

where $I_x = I_c \sin \theta_0 + \delta I_{clk}$. K_2 has been introduced to model any output buffer delay and $\phi(T_d)$ is defined by Eq. 7.

C. Modeling MTBF

Given the relationship between T_d and T_c , we can now derive the equations for the failure rate of a one-flop DFF synchronizer in the presence of a data pulse whose arrival times are uncorrelated to the clock input. We denote the timing slack at the output of the synchronizer under consideration as t_r . This is the maximum time after the clock pulse that the synchronizer output is allowed to generate an output pulse. In our experiments, we set t_r to be roughly 10% higher the nominal clock-to-Q delay of the DFF, as is typical in standard cell libraries [26]. Interestingly, if the predicted clock-to-Q delay exceeds the clock period t_{clk} , the output pulse appears earlier, directly after the next clock pulse, with negligible delay. This behavior does not cause any harm, because the handshaking protocol associated with synchronizers typically account for this potential increase in pulse latency [23].

Thus the probability of failure can thus be expressed as $p(\text{failure}) = p(t_r \leq T_c \leq t_{clk})$. Using Eq. 8, we obtain

$$p(\text{failure}) = p(f^{-1}(t_{clk}) \leq T_d \leq f^{-1}(t_r)) \quad (9)$$

The probability of failure is, thus equal to the probability of a pulse arriving in the window $\Delta T_d = (f^{-1}(t_{clk}) - f^{-1}(t_r))$ illustrated in Fig 2(a). Assuming a clock frequency of F_c and that the input data arrival time is uniformly distributed across the clock period, the probability of failure is

$$p(\text{failure}) = F_c * (f^{-1}(t_r) - f^{-1}(t_{clk})) \quad (10)$$

Assuming that the DFF is operating at a frequency of F_d , the total number of failures per second will be $F_c * F_d * (f^{-1}(t_r) - f^{-1}(t_{clk}))$. The MTBF of a single flop synchronizer is simply the reciprocal of this value,

$$MTBF = \frac{1}{F_c * F_d * (f^{-1}(t_r) - f^{-1}(t_{clk}))} \quad (11)$$

The addition of a second FF to the synchronizer decreases the size of this window, as illustrated in Fig. 2(b), increasing the MTBF. Note that our modeling approach is similar to the analysis of multistage CMOS synchronizers in [27] but our resulting equation is not closed-form. Finally we note that while MTBF grows rapidly as a function of the number of flip-flops the underlying function f is not an exponential, in contrast to CMOS [16], [28].

IV. SIMULATING METASTABILITY

The MTBF is a function of several device parameters that can be extracted from JSIM simulations of a DFF. This section describes our simulation results and curve fitting to estimate these parameters and the resulting MTBF of various flop synchronizers.

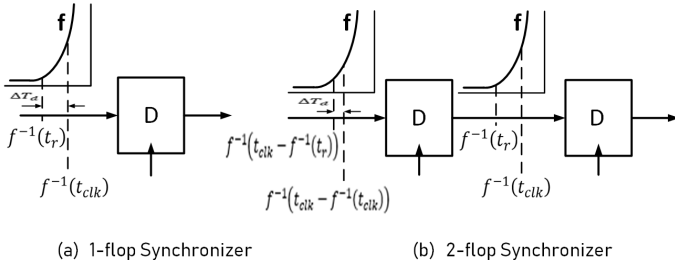


Fig. 2. Transition window for failure ΔT_d of (a) one-flop and (b) two-flop synchronizer

A. Simulation Setup and Results

To observe the relationship between T_d and T_c , we designed a custom DFF in the MIT LL $100\mu A/\mu m^2$ SFQ5ee process. We have kept t_{clk} equal to the highest clock-to-Q delay that the simulator exhibits (~ 39 ps) to maximize the number of data points in the steep region, near t_m , we give to our curve fitting program.

The dotted points in Fig. 3 show the simulation results of clock-to-Q delay T_c of our designed DFF as a function of the relative timing of the data pulse T_d . The curve on the top of the dotted points is obtained by curve fitting to Eq. 8. As we sweep T_d towards the clock pulse, we observe that the clock-to-Q delay starts to increase from $T_d = t_0$ until T_d reaches t_m where the flop no longer captures the input data pulse. We have refined the precision of t_m until T_d increments reach the minimum time difference that the simulator can resolve. Simulated values of t_0 , t_m and the setup time of our DFF (t_s) are shown in Fig. 3.

TABLE I
FAILURE WINDOWS AND MTBFs OF DIFFERENT SYNCHRONIZERS

Number of flops	Clock freq. F_c (GHz)	Failure transition window ΔT_d (ps)	MTBF
1	25	0.41	$0.039\mu s$
	30	0.405	$0.027\mu s$
	35	0.405	$0.02\mu s$
2	25	2.3×10^{-20}	$8.05 \times 10^9 yrs$
	30	5.3×10^{-12}	$1.8 \times 10^3 s$
	35	1.4×10^{-7}	$0.036s$

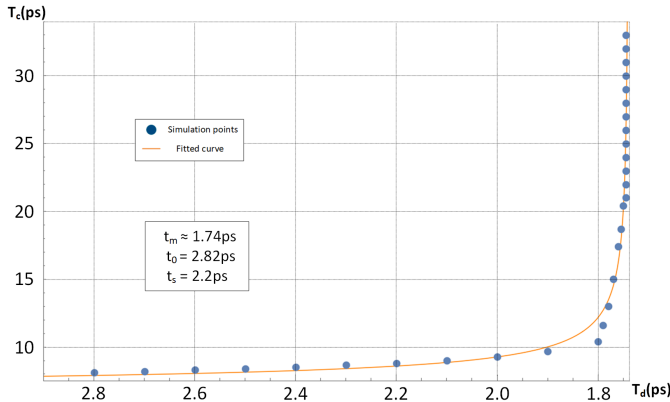


Fig. 3. Clock-to-Q delay (T_c) of a DFF as a function of the relative arrival time of the input pulse with respect to the clock (T_d). The dotted points indicate simulation results and the overlaid curve is the best fit of our proposed model.

B. MTBF Computation

To compute MTBF from Eq. 11, we used typical values of $F_c = 25$ GHz, $F_d = 2.5$ GHz and $t_r = 8$ ps. This is because the clock frequency of the current state-of-the-art SFQ processor is around 25 GHz [29] and we assume we have a data pulse once every ten clock cycles. We have kept t_r at 8 ps, because it is roughly 10% higher the nominal clock-to-Q delay of our DFF. To evaluate the function $f(T_d)$ as defined in Eq. 8, we set the values of I_c and R as used in our design and used curve fitting to estimate the other device parameters, namely I_1 , I_x , ϕ_0 , K_1 , and K_2 . This was motivated because I_1 , I_x , and ϕ_0 are difficult to otherwise evaluate and K_1 and K_2 involve non-linear effects that are not captured by our model. We ensured that the fitted values of these parameters are realistic. Our fitted function $f(T_d)$ has a Root Mean Square Error (RMSE) of 0.32 ps which is around 1% of the range of the dependent variable, T_c . RMSE is defined as

$$RMSE = \sqrt{\frac{\sum_{i=1}^n [t_{c_i} - f(t_{d_i})]^2}{n}} \quad (12)$$

and $(t_{c_i}, t_{d_i}) \forall i = \{1, 2, \dots, n\}$ are the n simulation points.

Plugging the assumed and fitted values described above in Eq. 11, we obtain an MTBF of $0.027\mu s$ for our one-flop synchronizer. Table I illustrates how we can improve this value by the addition of one more flop. Table I also describes the significant degradation in MTBF when the clock frequency F_c is increased.[†] For a clock frequency of 30 GHz, the MTBF of our two-flop synchronizer in the SFQ5ee process technology is estimated to be 8.05×10^5 years.

V. CONCLUSIONS

In this paper, we have derived an analytical model for metastability in SFQ from first principles from which we derived an equation for MTBF of DFF-based SFQ synchronizers. We applied this model to the MIT LL $100\mu A/\mu m^2$ SFQ5ee process by curve fitting our model to detailed JSIM simulations of a DFF designed in this process. The model fits our simulation results well showing low RMSE. Our model predicts that while a single DFF would lead to low MTBF, the standard back-to-back two-flop synchronizer, operating at 25 GHz, has an estimated MTBF of $\sim 10^6$ years.

Our future work includes the design of high-throughput synchronizers and demonstrating their use in large-scale SFQ designs. It would also be interesting to analyze the rate of growth of MTBF as a function of the number of flip-flops in an SFQ synchronizer and compare it to the standard exponential growth observed in CMOS.

VI. ACKNOWLEDGEMENT

The research is based upon work supported by the Office of the Director of National Intelligence (ODNI), Intelligence Advanced Research Projects Activity (IARPA), via the U.S. Army Research Office grant W911NF-17-1-0120. The views and conclusions contained herein are those of the authors and should not be interpreted as necessarily representing the official policies or endorsements, either expressed or implied, of the ODNI, IARPA, or the U.S. Government. The U.S. Government is authorized to reproduce and distribute reprints for Governmental purposes notwithstanding any copyright notation herein.

[†]As mentioned earlier, the data frequency (F_d) is always kept at 10% of the clock frequency.

REFERENCES

- [1] T. N. Theis and H.-S. P. Wong, "The end of moores law: A new beginning for information technology," *Computing in Science & Engineering*, vol. 19, no. 2, pp. 41–50, 2017.
- [2] K. K. Likharev and V. K. Semenov, "RSFQ logic/memory family: a new Josephson-junction technology for sub-terahertz-clock-frequency digital systems," *IEEE Transactions on Applied Superconductivity*, vol. 1, no. 1, pp. 3–28, 1991.
- [3] W. Chen, A. Rylyakov, V. Patel, J. Lukens, and K. Likharev, "Rapid single flux quantum T-flip flop operating up to 770 GHz," *IEEE Transactions on Applied Superconductivity*, vol. 9, no. 2, pp. 3212–3215, 1999.
- [4] D. S. Holmes, A. L. Ripple, and M. A. Manheimer, "Energy-efficient superconducting computing power budgets and requirements," *IEEE Transactions on Applied Superconductivity*, vol. 23, no. 3, 2013.
- [5] M. A. Manheimer, "Cryogenic computing complexity program: Phase 1 introduction," *IEEE Transactions on Applied Superconductivity*, vol. 25, no. 3, pp. 1–4, 2015.
- [6] O. A. Mukhanov, "Energy-efficient single flux quantum technology," *IEEE Transactions on Applied Superconductivity*, vol. 21, no. 3, pp. 760–769, 2011.
- [7] M. H. Volkmann, A. Sahu, C. J. Fourie, and O. A. Mukhanov, "Implementation of energy efficient single flux quantum digital circuits with sub-aJ/bit operation," *Superconductor Science and Technology*, vol. 26, no. 1, 2012.
- [8] Q. P. Herr, A. Y. Herr, O. T. Oberg, and A. G. Ioannidis, "Ultra-low-power superconductor logic," *Journal of Applied Physics*, vol. 109, no. 10, 2011.
- [9] M. Tanaka, M. Ito, A. Kitayama, T. Kouketsu, and A. Fujimaki, "18-GHz, 4.0-aJ/bit operation of ultra-low-energy rapid single-flux-quantum shift registers," *Japanese Journal of Applied Physics*, vol. 51, no. 5R, 2012.
- [10] N. Takeuchi, D. Ozawa, Y. Yamanashi, and N. Yoshikawa, "An adiabatic quantum flux parametron as an ultra-low-power logic device," *Superconductor Science and Technology*, vol. 26, no. 3, 2013.
- [11] P. Bunyk, K. Likharev, and D. Zinoviev, "RSFQ technology: Physics and devices," *International journal of high speed electronics and systems*, vol. 11, no. 01, pp. 257–305, 2001.
- [12] K. Gaj, Q. Herr, and M. Feldman, "Parameter variations and synchronization of RSFQ circuits," in *Conference Series-Institute of Physics*, vol. 148. IOP PUBLISHING LTD, 1995, pp. 1733–1736.
- [13] K. Gaj, E. G. Friedman, and M. J. Feldman, "Timing of multi-gigahertz rapid single flux quantum digital circuits," in *High Performance Clock Distribution Networks*. Springer, 1997, pp. 135–164.
- [14] Z. Al-bayati, O. Ait Mohamed, S. Rafay Hasan, and Y. Savaria, "Design of a C-element based clock domain crossing interface," in *2012-IEEE International Conference on Microelectronics*. IEEE, 2012.
- [15] D. Chen, D. Singh, J. Chromczak, D. Lewis, R. Fung, D. Neto, and V. Betz, "A comprehensive approach to modeling, characterizing and optimizing for metastability in FPGAs," in *Proceedings of the 18th Annual ACM/SIGDA International Symposium on Field Programmable Gate Arrays*, ser. FPGA 10. New York, NY, USA: Association for Computing Machinery, 2010, p. 167176. [Online]. Available: <https://doi.org/10.1145/1723112.1723142>
- [16] D. J. Kinniment and J. V. Woods, "Synchronisation and arbitration circuits in digital systems," *Proceedings of the Institution of Electrical Engineers*, vol. 123, no. 10, pp. 961–966, October 1976.
- [17] M. Thakur, B. B. Soni, P. Gaur, and P. Yadav, "Analysis of metastability performance in digital circuits on flip-flop," in *2014 International Conference on Communication and Network Technologies*, Dec 2014, pp. 265–269.
- [18] S. Tolpygo, V. Bolkhovsky, T. Weir, A. Wynn, D. Oates, L. Johnson, and M. Gouker, "Advanced fabrication processes for superconducting very large scale integrated circuits," *IEEE Transactions on Applied Superconductivity*, p. 11, 2016. [Online]. Available: <http://dx.doi.org/10.1109/TASC.2016.2519388>
- [19] E. S. Fang, "A Josephson integrated circuit simulator (JSIM) for superconductive electronics application," *Proc. Extended Abstr. Int. Supercond. Electron. Conf.*, pp. 407–410, 1989.
- [20] Q. P. Herr, D. L. Miller, and J. X. Przybysz, "Josephson comparator switching time," *Superconductor Science and Technology*, vol. 19, no. 5, pp. S387–S389, mar 2006. [Online]. Available: <https://doi.org/10.1088%2F0953-2048%2F19%2F5%2Fs46>
- [21] T. Filippov and M. Znosko, "Time characteristics of a Josephson-balanced comparator," *Superconductor Science and Technology*, vol. 12, no. 11, pp. 776–778, nov 1999. [Online]. Available: <https://doi.org/10.1088%2F0953-2048%2F12%2F11%2F325>
- [22] F. Wang and S. Gupta, "Automatic test pattern generation for timing verification and delay testing of RSFQ circuits," in *2019 IEEE 37th VLSI Test Symposium (VTS)*, April 2019, pp. 1–6.
- [23] G. Datta, H. Cong, S. Kundu, and P. A. Beerel, "Metastability-resilient synchronization FIFO for SFQ logic," 2019.
- [24] W. A. Clark, "Macromodular computer systems," in *Proceedings of the April 18-20, 1967, Spring Joint Computer Conference*, ser. AFIPS 67 (Spring). New York, NY, USA: Association for Computing Machinery, 1967, p. 335336. [Online]. Available: <https://doi.org/10.1145/1465482.1465536>
- [25] M. S. Hrishikesh, N. P. Jouppi, K. I. Farkas, D. Burger, S. W. Keckler, and P. Shivakumar, "The optimal logic depth per pipeline stage is 6 to 8 FO4 inverter delays," in *29th IEEE International Symposium on Computer Architecture*. IEEE, 2002, pp. 14–24.
- [26] N. K. Katam and M. Pedram, "Timing characterization for static timing analysis of single flux quantum circuits," *IEEE Transactions on Applied Superconductivity*, vol. 29, no. 6, 2019.
- [27] S. Beer, J. Cox, T. Chaney, and D. M. Zar, "Mtbf bounds for multistage synchronizers," in *Proceedings of the 2013 IEEE 19th International Symposium on Asynchronous Circuits and Systems*, ser. ASYNC 13. USA: IEEE Computer Society, 2013, p. 158165. [Online]. Available: <https://doi.org/10.1109/ASYNC.2013.18>
- [28] R. Ginosar, "Metastability and synchronizers: A tutorial," *IEEE Design Test of Computers*, vol. 28, no. 5, pp. 23–35, Sep. 2011.
- [29] Y. Yamanashi, M. Tanaka, A. Akimoto, H. Park, Y. Kamiya, N. Irie, N. Yoshikawa, A. Fujimaki, H. Terai, and Y. Hashimoto, "Design and implementation of a pipelined bit-serial SFQ microprocessor," *IEEE transactions on applied superconductivity*, vol. 17, no. 2, pp. 474–477, 2007.